# Aerosolized Hydrogen Peroxide Decontamination of N95 Respirators, with Fit-Testing and Virologic Confirmation of Suitability for Re-Use During the COVID-19 Pandemic

T. Hans Derr[1]*, Melissa A. James[2], Chad V. Kuny[4,7], Prem P. Kandel[5], Matthew D. Beckman[6], Kevin L. Hockett[5,7], Mark A. Bates[3], Moriah Szpara[4,7]*

[1] Environmental Health and Safety; [2] Animal Resource Program, [3] Occupational Medicine Program, and [4] Departments of Biology, Biochemistry and Molecular Biology, [5] Plant Pathology and Environmental Microbiology, [6] Statistics, [7] Center for Infectious Disease Dynamics, and the Huck Institutes of the Life Sciences, Pennsylvania State University, University Park, Pennsylvania 16802, USA

***Co-Corresponding Authors**

Moriah L. Szpara, PhD
Depts. of Biology, and Biochemistry & Molecular Biology
The Huck Institutes of the Life Sciences
Pennsylvania State University
W-208 Millennium Science Complex (MSC)
University Park, PA 16802 USA
Phone: 814-867-0008
Email: moriah@psu.edu

T. Hans Derr, CIH
Manager, Health & Environmental Programs
Environmental Health & Safety
Pennsylvania State University
6B Eisenhower Deck
University Park, PA 16802
Phone: 814-863-3834
Email: thd12@psu.edu

**Author emails:**

T. Hans Derr: thd12@psu.edu
Melissa A. James: maj22@psu.edu
Chad V. Kuny: cvk108@psu.edu
Prem Kandel: puk155@psu.edu
Matthew D. Beckman: beckman@psu.edu
Kevin L. Hockett: klh450@psu.edu
Mark A. Bates: mxb20@psu.edu
Moriah L. Szpara: moriah@psu.edu

# Abstract

In response to the current urgent demand for N95 respirators by healthcare workers responding to the COVID-19 pandemic, with particular emphasis on needs within local medical systems, we initiated an N95 decontamination study using aerosolized hydrogen peroxide or aHP (7% $H_2O_2$ solution), via the Pathogo Curis® (Curis) decontamination system. The study has thus far included 10 cycles of respirator decontamination, with periodic qualitative and quantitative fit testing to verify ongoing respirator integrity through the decontamination process, and support a statistical evaluation of successful respirator fit. In addition, we have conducted virologic testing of respirator surfaces and materials to demonstrate a rigorous verification of decontamination. Given that the current pandemic entails a respiratory viral pathogen, it is critical to address these aspects of respirator safety for reuse. These measures are intended to provide a foundation for a suitable decontamination process, which maintains N95 function, and supports safe respirator reuse by healthcare providers. Current results from both respirator fit testing and virologic testing indicate that the process is effective on the basis of zero failure rate on fit-testing of selected respirators, and on complete decontamination of multiple virus species by aHP treatment, comparable to that observed with commercial spore-based biological indicators of sterilization.


**Keywords:** N95 respirators, decontamination, aerosolized hydrogen peroxide, COVID-19, SARS-CoV2, virologic testing, virus, fit-testing, disinfection, sterilization

# Introduction

In response to the ongoing pandemic spread of Severe acute respiratory syndrome coronavirus 2 (SARS-CoV-2), there is a critical demand for personal protective equipment (PPE) to limit the spread of infection. In healthcare settings, the need for PPE is especially critical, to protect frontline healthcare providers from infection and to reduce cross-contamination between individuals with coronavirus disease 2019 (COVID-19) and those not yet infected. In healthcare settings, N95 respirators (including surgical N95 respirators) are frequently used to provide protection from airborne infectious particles. The N95 terminology for these respirators refers to their ability to block at least 95 percent of the most penetrating particle sizes (0.1 - 0.3 micron),

with increased efficiency for smaller or larger test particles. Proper use of N95 respirators requires qualitative or quantitative fit-testing, which are designed to ensure a tight face-to-respirator seal to the specific wearer's face.

The current COVID-19 pandemic has created a shortage of N95 respirators, due to limitations in manufacturing of critical components and in the ability of supply chains to handle increased global demand for PPE. For this reason, we and others have sought to demonstrate the potential for decontamination and reuse of existing N95 respirators. Standardized procedures already exist for the sterilization and reuse of medical equipment and surfaces, such as autoclaving, steam heat, and chemical inactivation (e.g. bleach) (1). Sterilization of most medical equipment is verified using spore-based biological indicators. Unlike most hospital equipment (e.g. steel, metal, plastic) or fabrics (e.g. blankets) for which standardized sterilization methods exist (1), N95 respirators were not intended for re-use (2). Thus many of the standard sterilization approaches deform, damage, or destroy the integrity of N95 respirator fabric, nosepieces, or elastic straps (3, 4). Aerosolized or vapor-phase hydrogen peroxide ($H_2O_2$) offers promising methods of use for decontamination for N95 respirators, with indications that these methods are non-deforming, non-damaging, and can penetrate the densely-woven fabric of respirator facepieces (3, 5). In addition, the virucidal capability of $H_2O_2$ sterilization methods have been previously demonstrated (6–8).

At present, respirator manufacturers have not approved protocols for respirator decontamination (2). However to address imminent pandemic needs, healthcare settings are referencing U.S. Centers for Disease Control and Prevention guidelines on provisional N95 respirator decontamination and reuse (9). Battelle Memorial Institute of Columbus, Ohio, recently received U.S. Food and Drug Administration (FDA) emergency use authorization for an N95 decontamination protocol using $H_2O_2$ vapor, based on a prior study addressing the potential for respirator reuse in emergency scenarios (3, 10). This prior Battelle decontamination study included evaluation of respirator structure, filtration and manikin fit-testing, and used bacterial spore-based biological indicators to demonstrate effective sterilization (3). It did not employ virologic testing, nor statistical evaluation of respirator fit on live subjects. Given that the current pandemic entails a respiratory viral pathogen, it is necessary to address these critical aspects of respirator safety for reuse. Due to the current urgency of COVID-19 pandemic, many

decontamination protocols are being investigated at research universities and medical centers (5, 11). The aerosolized hydrogen peroxide (aHP) method (e.g. Pathogo Curis® system) offers the advantage of using a lower level of $H_2O_2$ than comparable methods, such as vaporized $H_2O_2$ (VHP) systems using 30-35% $H_2O_2$, or those using 5% $H_2O_2$ in combination with silver (Ag) ions, which may leave toxic silver residue on respirator surfaces.

A demonstration study was conducted at the Pennsylvania State University at the Eva J. Pell Laboratory, to establish an effective N95 respirator decontamination protocol. This study focused on the ability of the Curis® decontamination system to effectively achieve viral and microbial sterilization of N95 respirators by aerosolized $H_2O_2$ (aHP), while preserving successful respirator fitting by medical staff after multiple cycles of decontamination. This study included multiple respirator facepiece types, representing those in wide use by local healthcare and research personnel. Successful decontamination of microbes was tested using stable, resistant spore-based bio-indicators (*Geobacillus stearothermophilus*), as well as by using multiple viral surrogates which represent the structure, characteristics, and environmental resistance of the SARS-CoV-2 pathogen. Virologic testing utilized sensitive plaque assays to detect the partial inactivation of viruses by drying onto respirator surfaces, and their subsequent decontamination by aHP. Fitness of respirators for reuse was assessed by qualitative and quantitative respirator fit testing on respirators subjected to multiple decontamination cycles. Real-time measurement and separate sample analyses were used to confirm acceptable aHP levels for decontamination, and the decomposition of aHP through drying prior to fit testing and reuse.

# Methods

## Curis® Decontamination Process (Decontamination Cycle)

The Curis® decontamination process was staged at the Eva J. Pell Biosafety Level 3 (BSL3) Laboratory, within in a 1,700 cubic feet Decontamination Room (Decon Room). The Decon Room includes solid surfaces which can be readily cleaned and sterilized. Filtered and conditioned air, with nominal control of humidity, is supplied to the Decon Room and the air exhausted from the room is HEPA filtered. Bubble tight dampers (Camfil Farr®) are used to seal both supply and exhaust air from associated ductwork in order to achieve neutral pressurization. Based on room volume, the standard recommended Curis® decontamination cycle includes:

under air-tight/sealed conditions, an approximate 12-minute continuous charge of aHP (7% $H_2O_2$; Curoxide®) was followed by six (6) pulse charges over 30 minutes. This was followed by an optional 15- or 20-minute air movement and circulation phase, under neutral pressurization and sealed room conditions, to increase disinfectant dwell time. An aeration or dissipation phase was then initiated after removing room seals for 30-minute to 2-hour periods, with the room under slight vacuum (0.18-0.19"W.G.), by starting the heating, ventilating, and air-conditioning (HVAC) equipment. Thereafter the respirator-holding rack(s) were transferred to a room (referred to as the "finishing room") with an HVAC air supply curtain to further dry and decompose residual aHP from respirator facepieces to less than 0.5 ppm $H_2O_2$ (7, 8). In order to optimize efficient aeration and dissipate detectable $H_2O_2$ from respirator facepieces, the cycle was monitored and parameters adjusted, including: air exchange rate, humidity, room temperature, and dwell time.

For respirators subjected to repeated rounds of decontamination as part of this study, decontamination cycles were conducted repetitively from staging through drying. In order to be considered "dry" or ready for the next cycle, the interior and exterior respirator surfaces were monitored using a calibrated, hand-held ATI PortaSens II (real-time $H_2O_2$ monitor), and $H_2O_2$ concentrations necessarily required to measure less than 0.5 ppm. Once this level was consistently achieved, respirators were then flexed bi-directionally, and each band was stretched twice to a hold position, while staged on the racks, prior to re-start of the next cycle.

## Monitoring of decontamination process

*Geobacillus stearothermophilus* spore coupons (Spordex®) (between 6 and 12 total per cycle) were placed throughout the room, and behind or beneath equipment and surfaces, and on portable metal racks holding respirators. These were collected after each cycle, transferred to growth media (Spordex® Culture Media), and analyzed after 7 days to ensure a 6-log reduction. Chemical indicator strips (between 1 and 4 total per cycle) were placed in strategic locations to indicate adequate $H_2O_2$ strength for successful decontamination. These were collected and analyzed after each cycle. An $H_2O_2$ Vapor [diffusion] Monitor (Assay Technologies, Model N587) was deployed to determine $H_2O_2$ peak, residual, and operator exposure concentrations during decontamination and simulated re-use process. This was achieved by clipping the monitor on the metal racks with respirators during the decontamination cycle (to verify concentrations),

on operator personnel (to monitor exposure levels), and in respirator bags (to monitor residual $H_2O_2$ before re-use in fit-testing). Laboratory analysis was performed by an American Industrial Hygiene Association-Accredited Laboratory. Separately, the PortaSens II detector was used to measure $H_2O_2$ levels during the charge/pulse stage of decontamination through a wall port in the room, and to monitor the adjacent corridor for room seal leakage. Subsequently it was used for direct measurements within the room itself during the aeration stage, and thereafter at respirator surfaces, to demonstrate $H_2O_2$ concentration reduction to less than 1 ppm for transport and to 0 ppm prior to fit testing.

## Selection of respirators for inclusion in the study

Several respirator models were included in the respirator fit-test process (**Table 1**). As a control to verify each respirator type could be fitted with the selected male and female subjects, non-decontaminated respirators were qualitatively fit-tested (QLFT) with subjects using the Occupational Safety and Health Administration (OSHA) qualitative fit test (QLFT) protocol (saccharine challenge) described at the OSHA Respiratory Protection Standard (29 CFR 1910.134) (12). This included several exercises to challenge respirator fit, over an approximate 8 minute, 30 second period. Additionally, quantitative fit-testing (QNFT) was conducted using OSHA protocol requirements using a T.S.I, Inc PortaCount Pro+ Model 8038 Fit Tester. This latter method employs condensation nucleus or particle counting technology (CNC or CPC) to measure aerosol concentration outside and inside the facepiece to determine a user fit-factor (13). Fit test administrators and subjects were significantly experienced as both test subjects and test administrators. Each subject achieved a 100% pass rate for all 3M respirator models, indicating good quality of fit, and successful fit-tests. One additional respirator model failed to pass QLFT by the female subject, and failed to pass QNFT by both male and female subject. Since this respirator model had a significant failure rate for both experienced subjects, it was removed from the fit-test study.

## Respirator Fit-Testing & Analysis

Prior to decontamination, respirators were labeled with a unique identifier. After decontamination, a hash mark was placed on the lower elastic band of each respirator to identify the round(s) of decontamination completed. At the conclusion of aHP decontamination described above, respirators were confirmed to have 0-0.5 ppm $H_2O_2$ (as monitored by PortaSens II) before

transfer to plain paper bags, within sealed plastic totes, and transport to the fit-testing facility. Since the study was conducted during the COVID-19 pandemic, social distancing conditions limited the use of multiple test subjects. Therefore two (2) respirator fit-test subjects were selected (one male, one female), to test successful fit for the selected respirators. All respirators were subjected to QLFT on the first, fifth, and tenth rounds of decontamination. In order to continually monitor QLFT test outcomes on the same facepieces over the course of sequential cycles of decontamination, only two of these were consumed by QNFT per model during each round of fit-testing. To conserve overall respirator use, respirators subjected to QNFT (with metal grommet in place from probe insertion) were returned for subsequent virologic testing.

## Mammalian virus inoculation and titration after drying or aHP decontamination

Prior to decontamination, respirator facepieces were inoculated with a controlled amount of one or more surrogate virus species (see **Table 2** for full list). Each virus was added in duplicate droplets of 10 μL each, on one or more surfaces of each respirator type. Droplets were allowed to air-dry or absorb onto each respirator in the open air flow of a biosafety cabinet. A sample of each virus-spotted facepiece was removed and left open to air, but without aHP decontamination, as a "dried" virus control. The remainder of each facepiece was subjected to aHP decontamination as described above (i.e. the "decontaminated" virus). After aHP, respirators were confirmed to have <1 ppm $H_2O_2$ before being transferred from the decon room to a cell culture facility for virus titration. At this stage each virus-inoculated location was sliced out of the "dried" or "decontaminated" respirators using dissection scissors. Each excised virus-spot encompassed all layers of the respirator, to capture any virus that had soaked below the surface fabric. Virus-inoculated respirator pieces were transferred into individual Eppendorf tubes and resuspended in a 250 μL volume of cell media. The number of infectious units, or plaque-forming units (PFU), of virus was determined by limiting dilution onto confluent Vero detector cell monolayers (*Cercopithecus aethiops* monkey kidney cells, ATCC® CCL-81™). Plaque formation was assessed at 72 hours post infection (hpi), after fixation and visualization of plaques using methylene blue staining. Duplicates of each virus-inoculated respirator piece were frozen for titration at a subsequent date, separate from the initial viral quantification. This allowed for experimental redundancy in terms of detector cell monolayers, and reduced handling time for the large numbers of virus-respirator inoculation sites.

### Bacteriophage Phi6 quantification

Inoculation of phi6 bacteriophage onto respirator facepieces followed the same approach as for other viruses (described above). However, phi6-inoculated respirator pieces were resuspended in 250 µL of King's medium B (KB). These were then quantified on lawns of *Pseudomonas syringae pathovar phaseolicola* strain 1448A (*Pph*) using a previously described soft agar overlay protocol (14). Briefly, 100 µl logarithmic culture of *Pph* ($OD_{600}$ ~ 0.5) and 100 µl of the phage preparation were sequentially added to 3 ml of molten soft agar (0.7%) maintained at 55ºC. The mixture was quickly poured on top of a KB agar plate and dried in the biosafety cabinet before transferring to a 28ºC incubator. Alternatively, for enumeration of "inoculum" and "dried" samples, soft agar *Pph* lawns were prepared and 10 µl dilutions of phage preparation were spotted. Plaque forming units (PFU) were enumerated after 24-48 hours of incubation at 28ºC.

## Results

### Selection of respirators for the study

The respirator facepiece models examined in this study represent those most frequently used at our institutions and local healthcare systems. These models include six types with a range of characteristics, including surgical N95 respirators (no exhalation valve to maintain sterile field), and non-surgical N95 respirators with an exhalation valve. These characteristics are summarized in **Table 1**, and illustrated visually in **Supplementary Figure 1**. In order to confirm respirator fitness for inclusion in this study, we first tested whether each respirator type could be fitted with experienced test subjects and test administrators. Several respirator models (listed in **Table 1**) were qualitatively fit-tested (QLFT) using Occupational Safety and Health Administration (OSHA) fit test protocols (see Methods for details) (12). We also carried out quantitative fit-testing (QNFT) using OSHA protocol requirements. QNFT employs condensation nuclei counting technology to measure aerosol concentrations outside and inside the facepiece to determine a user fit-factor. Five new respirators of each facepiece were subjected to QLFT, followed by QNFT. Successful QLFT and QNFT results were achieved for all five models of N-95 respirator facepieces shown in **Table 1**.

## Layout of respirator decontamination by aerosolized hydrogen peroxide (aHP)

Five models of respirator are presently utilized in this study, to gain insight into which models best withstand aHP and successfully complete fit-testing thereafter. Testing included more than 150 respirator fit-tests (see below for details). Wherever possible, respirators already subjected to quantitative fit-testing were redirected to virologic testing in future cycles, thus conserving overall respirator consumption for the study. Successful chemical disinfection by $H_2O_2$ was confirmed using Verify® Chemical Indicators ($H_2O_2$) placed on room surfaces, behind or beneath portable equipment in the decontamination room, and on the metal racks holding the respirators. Commercial spore-based biological indicators (*Geobacillus stearothermophilus)* were likewise placed on or between respirator facepieces on metal racks, as well as behind or beneath portable equipment in the decontamination room. These biological indicators confirmed complete spore killing by aHP. Respirator surface concentrations of residual $H_2O_2$ were monitored via a portable monitor. These ranged from non-detectable to <0.5 ppm aHP, prior to transfer for fit-testing or sealing for virologic testing. We found that respirator movement to a "finishing room" was useful to support more rapid $H_2O_2$ dissipation from respirators. While this study did not involve respirator reuse in actual hospital settings, we simulated conditions of reuse by handling respirators and stretching elastic between sequential decontamination cycles, in addition to wearing respirators during fit-testing as described below.

## Qualitative and quantitative fit-testing after aHP decontamination

Sequential fit-testing focused on a large number (>70) of the 3M 8511 model respirators. These were fit-tested after the first, fifth, and tenth cycles of decontamination, with one final round of fit-testing still to be completed after the fifteenth cycle. All respirators fit-tested were subjected to QLFT. In order to continually monitor QLFT test outcomes on the same facepieces over the course of sequential cycles of decontamination, only two of these were consumed by QNFT per model during each round of fit-testing. Respirators were split between the male and female subjects. Successful QLFT and QNFT were achieved on all respirators at each round tested thus far, for both the male and female subject. One respirator facepiece experienced a broken elastic strap after ten cycles of aHP, and thus failed fit-testing. No other failures have occurred. QLFT and QNFT was also conducted on a smaller number of additional respirator models (as indicated in **Table 1**, # included in study). For these respirator models, a maximum of 12 facepieces were

included, with all subjected to QLFT and typically two used for QNFT at the first, fifth, and tenth rounds. All respirators will be subjected to both QLFT and QNFT following the fifteenth cycle of decontamination. Subsequent similar testing is planned for one additional respirator model (70 respirators), to be subjected to 10 cycles of decontamination, with sequential rounds of fit-testing.

## Virologic Exam & Testing

Viral inactivation of inoculum on respirator facepieces was anticipated to occur both by the process of drying or desiccation, and by the process of aHP decontamination. Multiple virus species were selected as surrogates to test the decontamination potential of aHP against viruses in general, and against the characteristics of SARS-CoV2. To test the ability of aHP to inactivate viruses similar to this pathogen, we utilized two enveloped viruses, the RNA bacteriophage phi6, and the large DNA virus HSV-1. We also included the non-enveloped or naked-capsid enterovirus, CVB3. The key characteristics of the surrogate viruses, as compared to SARS-CoV-2, are summarized in **Table 2**.

Application of virus to each of five respirator facepiece types revealed clear differences in relative absorption vs. fluid repulsion. 3M respirator models 1870+ and 9211 share a common outer fabric which is listed by the manufacturer as having the highest fluid resistance of any N-95 respirator (15). In our testing, these two respirator models displayed no apparent absorption of virus inoculum in our tests, and instead dried with a "coffee ring effect" on the respirator surface. In contrast, all other respirator types (**Table 2**) experienced a combination of liquid spreading, absorption, and evaporation of the virus inoculum droplet. Virus was inoculated onto different areas of each respirator facepiece model, including the outer and inner fabric surfaces, the elastic strap, and where present, the inner and outer surface of the exhalation valves (see **Supplementary Figure 1**).

A sample of each virus-inoculated facepiece was left open to air, without aHP decontamination, as a "dried" virus control. The remainder of each virus-inoculated facepiece was treated with aHP for decontamination, and the virus-spotted areas were collected and tested for infectiousness thereafter (**Figure 1**). The "dried" samples confirmed a partial loss of viral infectiousness for HSV-1 (e.g. $10^6$ PFU input vs $10^5$ PFU after drying) and CVB3 (e.g. $10^4$ PFU input vs $10^2$ PFU

after drying), with only a minimal effect on phi6 (e.g. $10^7$ PFU for input and after drying). The samples subjected to aHP decontamination appeared to have no infectious virus remaining in 55 of 58 samples tested. The only positive viral plaques to occur after aHP decontamination occurred in parallel with failure of a spore-based biological indicator, as described below. The effects of drying and inactivation did not vary substantially by either the respirator surface or location being tested, or the brand and model of respirator. No plaques were detected in the duplicate viral-spotted samples of any aHP- decontaminated respirators, for any of the three viral species.

During optimization of the aHP dwell time parameter, one cycle of aHP decontamination experienced a failure on 1 of 6 spore-based biological indicators placed in the room (see Methods). On this date, there were also three samples in which either 1 or 2 viral plaques were detected (HSV-1 and CVB, respectively). These points are denoted in red **Figure 1**, and are likewise shown as plaques in **Supplementary Figure 2**. No plaques were detected in the duplicate samples of these inoculation sites, suggesting that these were either rare infectious particles or these were inactivated by freezing prior to plating of the duplicate samples. These were the only occasions on which any infectious units of any virus species were observed after aHP decontamination. Due to failure of the spore-test on that aHP cycle, respirators from this failed decontamination cycle would not have been entered into further use in a healthcare setting. Together these data suggest that the use of commercial spore-based biological indicators during decontamination of N95 respirators provides a useful predictor of success or failure in viral decontamination as well.

# Discussion

Based on a series of ten respirator decontamination cycles thus far, which to date have included two rounds of virologic testing, we found successful respirator decontamination by aHP and fitness for respirator reuse in this pilot study. We found that respirators were not substantively degraded (chemically or physically) by multiple cycles of aHP, as reflected in successful fit testing throughout the decontamination process. We used intentional viral inoculation onto specific respirator surfaces to thoroughly test for the ability of aHP to inactivate viruses, and to discern whether any differences in respirator construction (e.g. outer vs. inner surface fabric)

would influence viral inactivation. We found no evidence of viral survival of aHP decontamination. During optimization of $H_2O_2$ dwell-time parameters, we found that during a failed decontamination cycle both commercial spore-based biological tests and intensive virologic testing failed in synchrony. This suggests that medical facilities seeking to use aHP decontamination protocols can rely on spore-based methods to confirm sterilization, making this technology widely applicable beyond those with facilities capable of performing virologic testing. In ongoing work on this pilot study, we plan to maximize rigor by evaluating of up to 15 rounds of decontamination, which is the maximum use advised by the US FDA for the Battelle Decontamination VHP protocol (3, 10).

Like SARS-CoV-1, SARS-CoV-2 has a high level of environmental stability (16–20). In terms of virion characteristics, SARS-CoV-2 has a lipid enveloped virion of ~120 nm, with no icosahedral capsid core. The lipid envelope encloses a single-stranded, linear, positive-sense RNA genome (summarized in **Table 2**). We used multiple virus species to test the viral inactivation capabilities of aHP decontamination. These viruses represented multiple characteristics of human viral pathogens, with a range of virion types and sizes, genome types and lengths, and previously documented environmental stability (21–23). Virions of herpes simplex virus 1 (HSV-1) and *Pseudomonas* phi6 bacteriophage have a lipid envelope, with an underlying icosahedral capsid core. In contrast, coxsackievirus B3 (CVB3) is a non-enveloped or naked icosahedral capsid virus. Prior work has shown that naked-capsid viruses have a higher stability than enveloped viruses, thus providing a useful test of aHP sterilization abilities (21–23). While most viruses utilized in this study are mammalian viruses requiring analysis in mammalian cell lines at biosafety level 2 (BSL2), phi6 can be assayed more flexibly, using rapid bacterial cultures (24-hour turnaround) at biosafety level 1. Phi6 is a natural pathogen phage of *Pseudomonas syringae pathovar phaseolicola*, which is itself a bacterial pathogen of green beans. We found that all viral species examined in this study were effectively sterilized by aHP, comparable to the decontamination observed with commercial spore-based biological indicators of sterilization. Together, this combination of respirator fit testing and virologic testing suggest that aHP is a suitable decontamination process to enable reuse of N95 respirators during the COVID-19 pandemic.

## Acknowledgements

This work was supported by the Pennsylvania State University. We appreciate the contributions of colleagues and scientists who provided intellectual input and/or reagents for this work. These include Dr. Joyce Jose, Dr. Troy Sutton, Dr. Tony Schmitt, James Crandall, and Dr. Michael Brignati, JD. We appreciate the contributions of the expert Environmental Health and Safety staff involved in study design, implementation and fit-testing, and the healthcare providers of the Penn State Health Milton S. Hershey Medical Center and College of Medicine.

# Tables

### Table 1: N-95 Respirator facepiece models included in this study.

| Brand & model | # included in study | Type | Exhalation valve | Notes |
|---|---|---|---|---|
| 3M 8511 | 77 | Non-surgical | yes | |
| 3M 1860 | 10 | Surgical | no | |
| 3M 1870+ | 11 | Surgical | no | Highest fluid resistance* |
| 3M 9211+ | 12 | Non-surgical | yes | Same fabric as 1870+ |
| Honeywell Sperian N11125 | 5 | Non-surgical | yes | |

* Highest level of fluid resistance according to ASTM F1862 at 160 mm Hg (15).

### Table 2. Characteristics of virus species used to test inactivation by aerosolized $H_2O_2$, as compared to SARS-CoV-2.

| Virus species (abbreviation) | Diameter | Capsid / virion shape | Genome type, ~size* | Taxonomic family |
|---|---|---|---|---|
| Severe acute respiratory syndrome coronavirus 2 (SARS-CoV-2) | 120 nm | Enveloped, no icosahedral capsid | linear (+) ssRNA genome, ~30 kbp | *Coronaviridae* |
| Herpes simplex virus 1 (HSV-1) | 200 nm | Enveloped, icosahedral | linear dsDNA genome, ~152 kbp | *Herpesviridae* |
| Coxsackie virus B3 – CVB3 | 30 nm | Non-enveloped (naked), icosahedral | linear (+) ssRNA genome, ~7.4 kbp | *Picornaviridae* |
| *Pseudomonas* phi6 bacteriophage | 85 nm | Enveloped, icosahedral | segmented, dsRNA genome, ~13.3 kbp | *Cystoviridae* |

*ss, single-stranded; ds, double-stranded; (+), positive sense; (-), negative sense.

# Figure Legends

**Figure 1** (legend follows image)

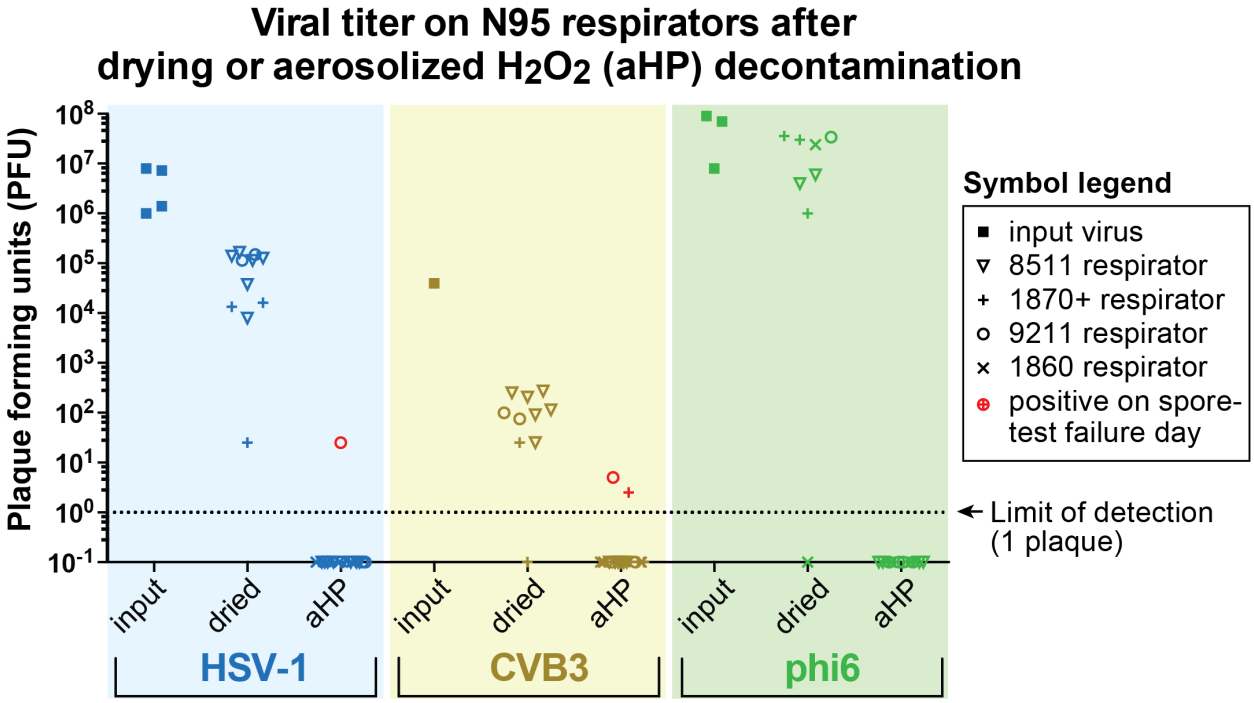


**Figure 1: Viral titer on N95 respirator facepieces was reduced after drying and eliminated after aerosolized $H_2O_2$ (aHP) decontamination.** Multiple models of N95 respirator (see legend above, and **Table 1** for respirator details) were inoculated with each of three viral species. These viruses represent a range of virion types and characteristics (see **Table 2** for virus details), thus demonstrating the relative ability of aHP to inactivate many different viruses. The input inoculum for each virus was set to the maximum available in each viral stock preparation. HSV-1 and CVB3 showed a greater loss of infectiousness (plaque forming units, or PFU) due to drying than phi6. All virus species were inactivated by aHP. During optimization of aHP procedures, one cycle with short dwell time resulted in a failure of commercial spore-based biological indicators; indicating that aHP levels did not reach a sufficient level for full decontamination on that cycle. On this day 3 virus-inoculated sites were also positive (plotted in red, for ease of comparison), although other viral spots were still inactivated by the partial $H_2O_2$ decontamination. The dashed horizontal line indicates the limit of detection at 1 viral plaque. For the purposes of illustrating the disinfected samples where zero plaques were detected, these numbers were replaced with fractional values (e.g. 0.1), to allow their visualization on the log-scale plot.

# References

1. Rutala WA, Weber DJ, Healthcare Infection Control Practices Advisory Committee (HICPAC). 2008. Guideline for Disinfection and Sterilization in Healthcare Facilities, 2008. Cent Dis Control CDC 163.

2. 3M Personal Safety Division. 2020. Disinfection of Filtering Facepiece Respirators. 3M Tech Bull 4.

3. Battelle Memorial Institute. 2016. Final Report for the Bioquell Hydrogen Peroxide Vapor (HPV) Decontamination for Reuse of N95 Respirators. Prep Contract – Study Number 3245 US Food Drug Adm 46.

4. Liao L, Xiao W, Zhao M, Yu X, Wang H, Wang Q, Chu S, Cui Y. 2020. Can N95 respirators be reused after disinfection? And for how many times? preprint, Occupational and Environmental Health.

5. Schwartz A, Stiegel M, Greeson N, Vogel A, Thomann W, Brown M, Sempowski GD, Alderman TS, Condreay JP, Burch J, Wolfe C, Smith B, Lewis S. 2020. Decontamination and Reuse of N95 Respirators with Hydrogen Peroxide Vapor to Address Worldwide Personal Protective Equipment Shortages During the SARS-CoV-2 (COVID-19) Pandemic. Appl Biosaf 153567602091993.

6. Goyal SM, Chander Y, Yezli S, Otter JA. 2014. Evaluating the virucidal efficacy of hydrogen peroxide vapour. J Hosp Infect 86:255–259.

7. Tuladhar E, Terpstra P, Koopmans M, Duizer E. 2012. Virucidal efficacy of hydrogen peroxide vapour disinfection. J Hosp Infect 80:110–115.

8. Holmdahl T, Odenholt I, Riesbeck K, Medstrand P, Widell A. 2019. Hydrogen peroxide vapour treatment inactivates norovirus but has limited effect on post-treatment viral RNA levels. Infect Dis 51:197–205.

9. 2020. CDC - Recommended Guidance for Extended Use and Limited Reuse of N95 Filtering Facepiece Respirators in Healthcare Settings - NIOSH Workplace Safety and Health Topic.

10. Hinton, Chief Scientist, Food and Drug Administration D. 2020. FDA Letter - Emergency Use Authorization (EUA) for the Battelle Critical Care Decontamination System (CCDS).

11. Kenney P, Chan BK, Kortright K, Cintron M, Havill N, Russi M, Epright J, Lee L, Balcezak T, Martinello R. 2020. Hydrogen Peroxide Vapor sterilization of N95 respirators for reuse. preprint, Infectious Diseases (except HIV/AIDS).

12. Occupational Safety and Health Administration (OSHA), United States Department of Labor. Fit Testing Procedures (Mandatory). 1910134 App A.

13. Operation and Service Manual. 2015. Portacount Pro 8030 and Portacount Pro+ 8038 Respirator Fit TestersRev. P. T.S.I., Inc., Shoreview, MN.

14. Hockett KL, Baltrus DA. 2017. Use of the Soft-agar Overlay Technique to Screen for Bacterially Produced Inhibitory Compounds. J Vis Exp.

15. 3M Personal Safety Division. 3M™ Aura™ Health Care Particulate Respirator and Surgical Mask 1870+, N95.

16. van Doremalen N, Bushmaker T, Morris DH, Holbrook MG, Gamble A, Williamson BN, Tamin A, Harcourt JL, Thornburg NJ, Gerber SI, Lloyd-Smith JO, de Wit E, Munster VJ. 2020. Aerosol and Surface Stability of SARS-CoV-2 as Compared with SARS-CoV-1. N Engl J Med.

17. Sizun J, Yu MWN, Talbot PJ. 2000. Survival of human coronaviruses 229E and OC43 in suspension and after drying onsurfaces: a possible source ofhospital-acquired infections. J Hosp Infect 46:55–60.

18. Duan S-M, Zhao X-S, Wen R-F, Huang J-J, Pi G-H, Zhang S-X, Han J, Bi S-L, Ruan L, Dong X-P, SARS Research Team. 2003. Stability of SARS coronavirus in human specimens and environment and its sensitivity to heating and UV irradiation. Biomed Environ Sci BES 16:246–255.

19. Rabenau HF, Cinatl J, Morgenstern B, Bauer G, Preiser W, Doerr HW. 2005. Stability and inactivation of SARS coronavirus. Med Microbiol Immunol (Berl) 194:1–6.

20. Geller C, Varbanov M, Duval R. 2012. Human Coronaviruses: Insights into Environmental Resistance and Its Influence on the Development of New Antiseptic Strategies. Viruses 4:3044–3068.

21. Firquet S, Beaujard S, Lobert P-E, Sané F, Caloone D, Izard D, Hober D. 2015. Survival of Enveloped and Non-Enveloped Viruses on Inanimate Surfaces. Microbes Environ 30:140–144.

22. Kampf G, Todt D, Pfaender S, Steinmann E. 2020. Persistence of coronaviruses on inanimate surfaces and their inactivation with biocidal agents. J Hosp Infect 104:246–251.

23. Vasickova P, Pavlik I, Verani M, Carducci A. 2010. Issues Concerning Survival of Viruses on Surfaces. Food Environ Virol 2:24–34.

# Supplementary Figure Legends

**Supplementary Figure 1** (legend follows image)

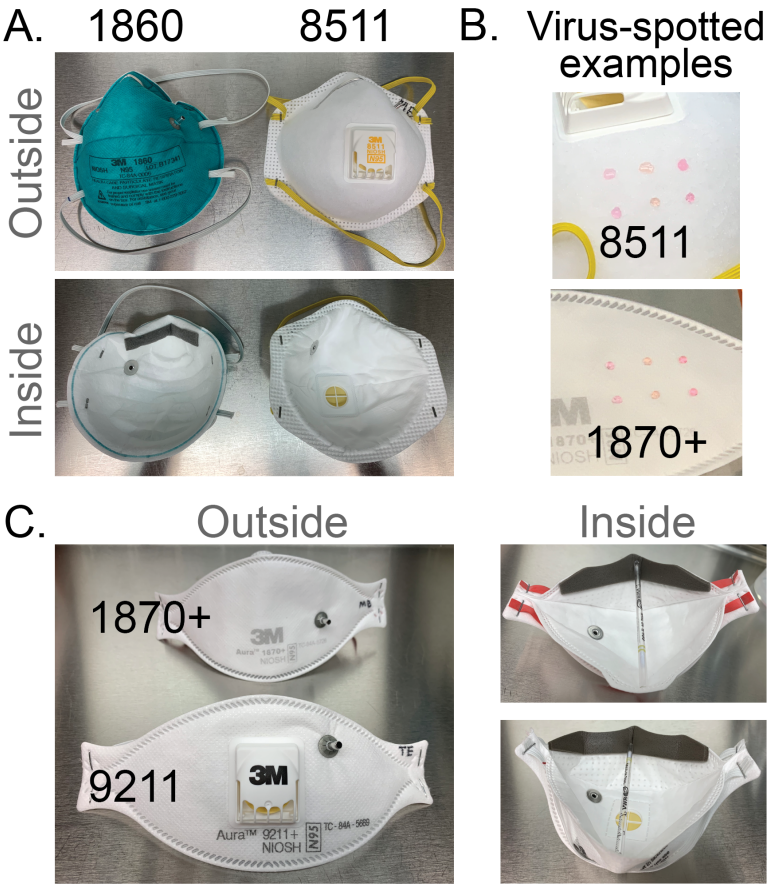


**Supplementary Figure 1: Respirator Facepieces included in this study demonstrate a range of models and characteristics. (A)** 3M models 1860 and 8511 (left) have a molded facepiece, with 8511 including an exhalation valve. **(B)** Virus-inoculation via droplets spotted onto the respirator fabric are shown for two examples. **(C)** 3M models 1870+ and 9211+ share a common folded fabric model, with a high fluid resistance of the fabric. 3M 9211+ includes an exhalation valve. Several of the facepieces (1860, 1870+, 9211+) display the metal grommet from insertion of the probe used for quantitative fit testing (QNFT). The inner face of each respirator is shown, which for the models shown in **(C)** required a prop to hold them open.

**Supplementary Figure 2** (legend follows image)

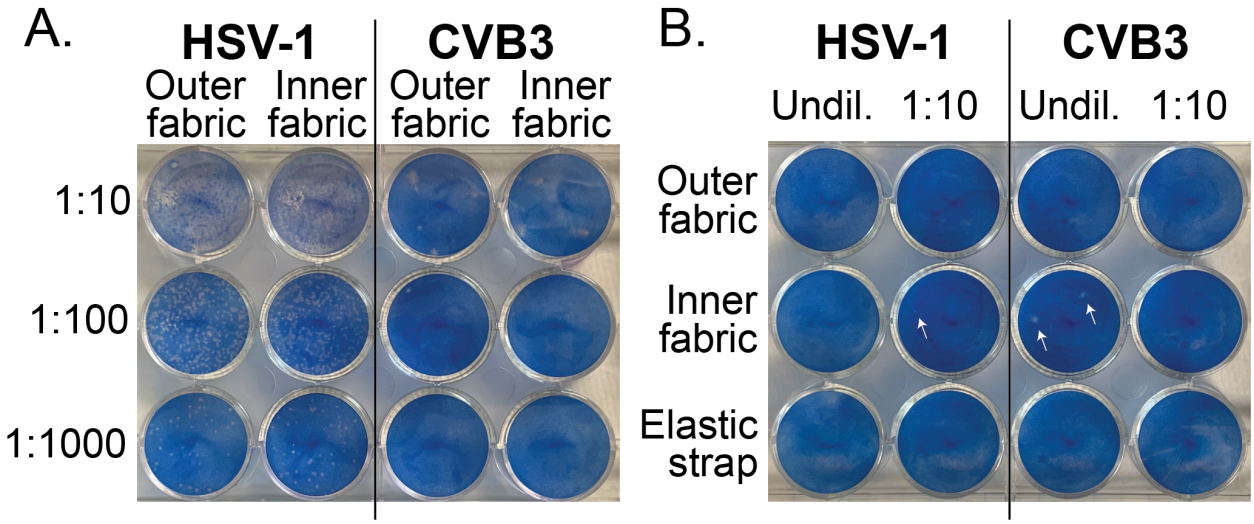


**Supplementary Figure 2: Viral titration demonstrates inactivation and loss of infectious units due to drying and aerosolized $H_2O_2$ (aHP) decontamination.** Shown here are representative examples of serial dilutions (titration) of HSV-1 or CVB3 that were spotted onto 3M 9211 respirators, and then resuspended and plated onto monolayers of Vero detector cells. Viral plaques, which are visible as clear foci of infection (plaque-forming units, or PFU) on the background of methylene blue-stained cells, were visualized at 72 hours post infection. The plate shown in **(A)** illustrates titration of a high concentration of HSV-1 after drying ($10^5$ PFU), and a lower concentration of CVB3 after drying ($10^2$ PFU; see **Figure 1** for titer data). The plate shown in **(B)** is from the one aHP cycle when dwell time was short and commercial spore-based biological indicators indicated a failure of decontamination. Even on this partial aHP decontamination, only three wells (of which two are shown above) had any viral plaques (indicated by arrowheads; these equate to 25 PFU of HSV-1, and 5 PFU of CVB3). All cycles with successful inactivation of spore-based biological indicators by aHP had complete viral inactivation as well (e.g. top and bottom rows of plate shown in **(B)**). In contrast, drying on respirators facepieces without aHP **(A)** only partially inactivates these viruses.

**Supplementary Figure 3** (legend follows image)

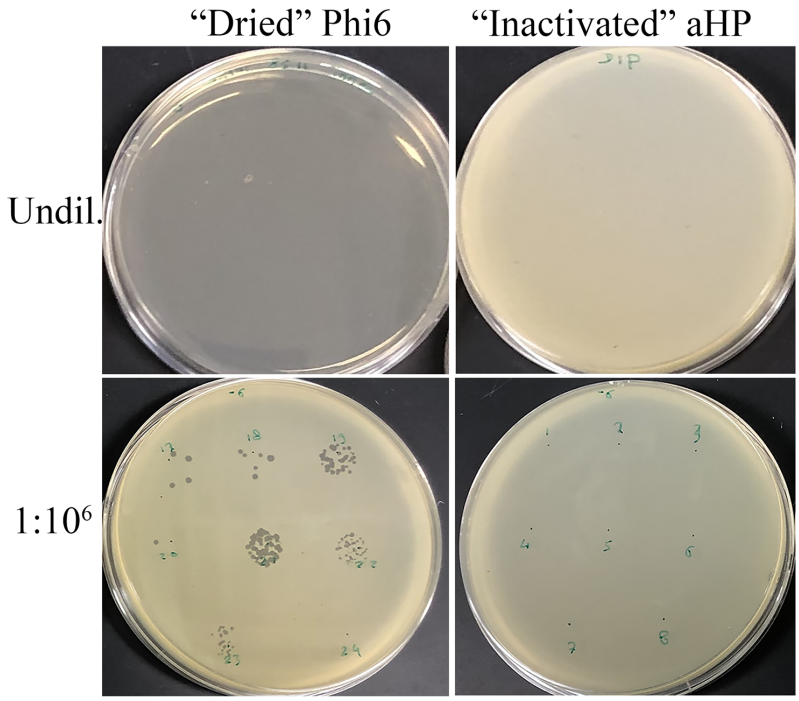


**Supplementary Figure 3: Bacteriophage phi6 titration after drying or aerosolized $H_2O_2$ (aHP) decontamination demonstrates inactivation and loss of viral infectious units.** Shown here are representative examples of soft agar lawns of the phi6 host bacteria, *Pseudomonas syringae pathovar phaseolicola.* Resuspensions of phi6 from dried or aHP-treated respirators were either plated onto bacterial lawns in undiluted form (top), or diluted $1{:}10^6$ and spotted onto intact bacterial lawns (bottom). The upper left plate shows complete bacterial lysis by phi6, since its titer was largely unaffected by drying (see **Figure 1**). In contrast, the bacterial lawn is thick and unmarred by any phi6 plaques after aHP decontamination. In the diluted phi6 resuspensions on the bottom row, numbered spots delineate phi6 resuspensions from individual respirator types and facepiece locations (see **Figure 1** for all data).